P2.15 SURFACE TEMPERATURES AND WINDS OVER COMPLEX TERRAIN: OBSERVATIONS AND MM5 MESOSCALE MODEL SIMULATIONS

D. Rostkier-Edelstein[1], S. Berkovic, and R. Givati
Israel Institute for Biological Research

1. INTRODUCTION

During the last decades mesoscale models have become an attractive tool to predict meteorological variables at high horizontal and vertical resolutions in support of operational weather forecasting and air quality monitoring and assessment. In particular, coastal complex terrain regions constitute challenging areas for meteorological and air quality modeling. Mesoscale air flow in these regions is determined by the land-sea temperature contrast (land-sea breeze), the topography and the shape of the coastline.

This paper presents preliminary results of a project with a twofold aim: 1. To test the ability of the Penn State/NCAR MM5 mesoscale model to reproduce the major features of the flow in a coastal area of complex terrain in Israel; 2. To statistically evaluate the model results versus observations (as opposed to a specific episode reproduction). The evaluation is done by comparison of simulated and observed surface winds and temperatures. We stress the importance of the present type of evaluation when simulated meteorological variables are to be used as input to air quality models. To the best of our knowledge this is the first evaluation of this kind of MM5 model results at high resolution over Israel. We emphasize that the results presented here reflect the performance of the model run in a particular configuration and suggest changes for further optimization.

The outline of this paper is as follows: In Sec. 2 we present the topography of the studied area; Sec. 3 describes briefly the major characteristics of the synoptic and mesoscale flow during the simulated period; Sec. 4 summarizes the specific details of the MM5 model simulations; In Sec. 5 we analyze the observations and MM5 model results and compare between them; Sec. 6 summarizes the study and suggests further approaches to improve the evaluation techniques and model results.

2. TERRAIN OF THE STUDIED AREA

Fig.1 shows the studied area as resolved by the 2 km resolution grid used in our simulations (see Sec. 4) and the location of the surface stations. The topography is characterized by: 1. The sea to the west of the lowest countour. 2. A ridge with a slope of about 26 m/km rising from northwest to southeast, i.e., from the cape inland; 3. A coastal plain northern of it; 4. A very shallow valley to the east and to the south. The surface observation stations may be classified into three categories: 1. Stations on the ridge and on its slope (numbers 1, 3, 5 and 6); 2. Coastal plain stations (numbers 4 and 8); and 3. Inland stations (numbers 2 and 7). This classification will be useful in our further analysis. All stations are located in urban areas at a height of about 6 to 10 meters above the roofs.

[1]Corresponding author address: Dorita Rostkier-Edelstein, Dept. of Math., IIBR, POB 19 Ness-Ziona 74100 Israel
Email: rostkier@iibr.gov.il

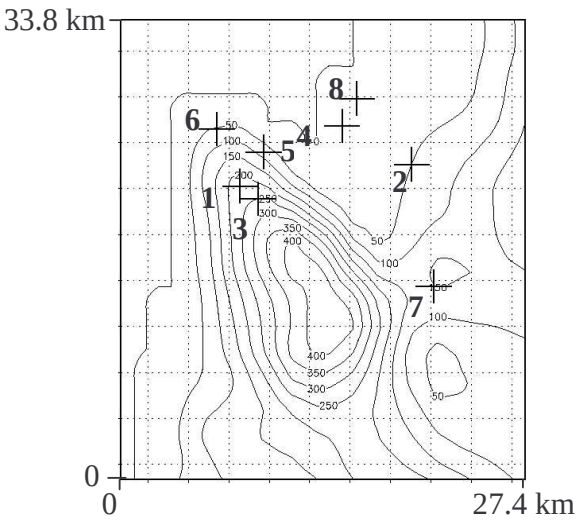

Fig. 1: Topography of the studied area and location of the surface observation stations

3. SYNOPTIC AND MESOSCALE BACKGROUND

Our study focused on a summer period. Throughout the summer, the eastern Mediterranean is dominated by a Subtropical ridge extending from the north-African coast to the east, and by the Persian trough extending from the monsoonal low through the Persian Gulf to the northeast Mediterranean and Turkey (see e.g. Alpert et al., 1992). The synoptic induced near surface wind direction is westerly and during the day hours it rather overlaps with the direction of the sea-breeze, therefore, resulting in a westerly to north-westerly wind flow of nearly 7 m/s. During the night the influence of the easterly oriented land-breeze is quite similar to that of the synoptic system (but opposite in its direction), the synoptic flow weakens the land-breeze and slightly deviates it, resulting in a wind flow from the south at about 2.5 m/s. The sea-breeze mechanism along the Mediterranean coast of Israel has been studied during the last decades (Doron and Neumman, 1977; Alpert et al., 1982; Lieman and Alpert, 1993; Khain et al., 1993). It is specially pronounced in summer, when land-sea temperature gradients attain their maximum. In addition to the synoptic flow, the westerly oriented sea-breeze is enhanced by the anabatic winds along the mountainous regions inland. Some researches have even considered the nocturnal land-breeze along the Mediterranean Israel coast as a mountain breeze rather than a land breeze (Doron and Neumman, 1997). A comprehensive summary of the factors affecting the sea-breeze development may be found in Arrit, 1989.

4. MODEL SETUP

The PSU/NCAR mesoscale model, MM5, version 3.2, was configured using 4 nested domains with 1 way nesting interaction and with horizontal resolutions of 54, 18, 6 and 2 km (Fig. 2). The vertical resolution is of 26 levels with 11 levels between sigma 1.0 and 0.8. Forty-eight hour simulations initialized at 0 UTC were run for July 1994. The model employed the following physical options: 1) Grell cumulus scheme, 2) MRF boundary layer scheme, 3) Five-layer soil temperature model, 4) Dudhia simple ice microphysical scheme, and 5) Cloud-radiation scheme. The first guess and boundary conditions were provided from the GEOS-1 Multi Year Assimilation Data Mediterranean subset (at NASA-EOSDIS, Tel-Aviv University, Da-Silva and Alpert, 1996), with spatial resolution of 2° latitude by 2.5° longitude and temporal resolution of 6 hours; and from the AVHRR sea surface temperature data set, with spatial resolution of 0.5° latitude and longitude and averaged over 5 days (WOCE Satellite Data CD-ROM, Version 1.1). No objective

analysis or data assimilation was done. As stated in Sec. 2 all stations are located in urban areas. The urban character of the area is modeled by means of urban land use characteristics as defined in MM5 model and no urban surface layer or planetary boundary layer parameterization were included. Fig. 3 shows the land use as resolved by the 2 km resolution MM5 domain. This figure displays also the coastline as resolved at the 2 km model resolution.

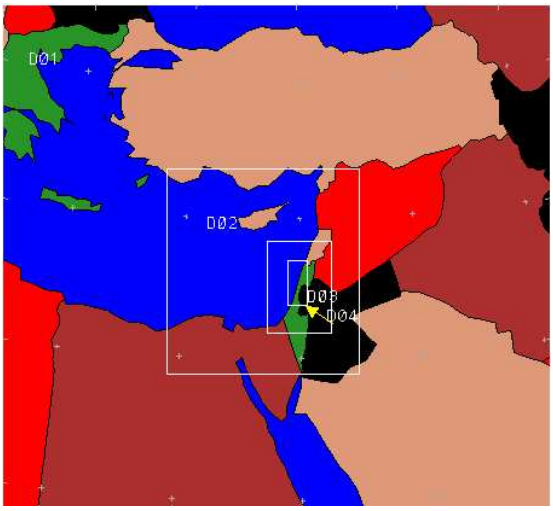

Fig. 2: 54, 18, 6 and 2 km MM5 modeling domains.

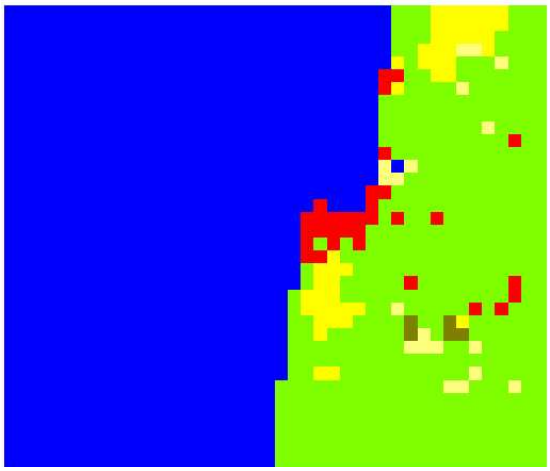

Fig. 3: Land use categories as resolved by the 2km resolution MM5 domain. Red: urban. Blue: water. Other colors: rural.

5. MODEL EVALUATION

Model variables were output every hour. 10 minutes averaged observations of wind and temperature, collected during July 1994, at model output times were used for the evaluation. The evaluation is performed by comparison of simulated and observed monthly averaged daily cycles of temperatures and wind speeds, wind speed and wind direction distributions and monthly averaged hourly wind vectors. The model output at 2 km resolution and about 15 m above the surface, after 24 hours of spin up, is presented for comparison. We emphasize that the evaluation is done for each of the stations independently, and not averaged over the whole set, in order to test the validity of the model in different terrain areas.

5.1. Monthly averaged daily cycles of temperatures.

The most significant changes in the near surface temperature are caused by the daily heating-cooling cycle. The amplitude of the cycle reaches its maximum during the summer. As stated before, the daily heating-cooling mechanism is responsible for the sea-land breeze cycle and for mountain anabatic and katabatic winds during the day and night respectively.

Fig. 4 shows the observed and simulated monthly averaged diurnal cycle of the temperature for six of the stations (no temperature measurements were collected at stations 5 and 8). Results will be analyzed by means of the amplitude and timing of the diurnal cycle. The main features may be summarized as follows:

1. Both observations and simulations show that stations at high elevations on the ridge (1, 3 and 6) exhibit the smallest

amplitudes, of about 3°. There are several reasons for that. During the heating hours the ground is heated and the temperature of the air diminishes with height. Stations at high elevation sites, 1 and 3, receive advected cooler air from relatively higher levels resulting in an advection cooling effect. Station 6 shows a similar pattern, however shifted to higher temperatures both during the day and the night. This is a result of the proximity to the sea, which tends to diminish cooling during the night, and of the lower terrain elevation, which gives rise to higher temperatures during the day.

2. Observations and simulations reveal a similar timing pattern in stations 1, 3 and 6 characterized by a short heating period during the morning, a result of the early penetration of the sea-breeze, followed by an almost constant temperature period until the afternoon hours when solar heating weakens.
3. The largest amplitudes of about 9° are observed at the inland stations 2 and 7. This is a consequence of the distance from the coast and delay of the sea-breeze penetration, which allows heating to continue until noon. Simulated results also show maximal amplitudes at these stations, but smaller than the observed (about 6.5° and 5.5° in stations 7 and 2 respectively). In particular, we emphasize the lower simulated maximum temperature, by about 3°, at station 2.
4. In spite of the similar observed amplitudes at stations 2 and 7, rather different timing patterns are found: the maximum temperature is reached at station 7 about two hours later than at station 2, and the cooling slope is shallower in station 2. This behavior is a result of their location relative to the coast and the topography: the sea-breeze reaches station 2 by midday and weakens solar heating, while station 7, farther from the coast and behind the ridge, starts to cool down only in the afternoon. The model reproduces quite well the temperature cycle timing at station 2 but fails to correctly simulate the behavior at station 7 as the simulated temperature maximum appears two hours earlier than observed.
5. Observations at station 4 show an intermediate behavior as compared to the two groups of stations discussed above: an amplitude of 6°, maximum temperature at midday and higher temperatures than the previous stations at night and early morning hours. This is a consequence of the proximity to the sea and of the flat topography, which weakens cooling at night and heating during the day as explained above. However, simulations show a different timing pattern: warming slows down early in the morning (around 8 am) as seen in stations 1, 3, and 6. This discrepancy indicates possibly different dynamics developing in the observations and in the model. We should keep in mind the coarse resolution of the coastline by the model (Fig. 3).

6. Minimum averaged temperatures are found in all stations at 5 am both in observations and simulations.

5.2. Wind direction and wind speed distributions.

Fig. 5 shows the simulated and observed joint distribution of wind directions into octants and of wind speeds into five categories for the eight stations. Results may be summarized as follows.

1. Both observations and model results show that the flow is dominated by winds blowing from the south, south-west, west and north-west octants. Winds from other sectors are infrequent as expected from the synoptic and mesoscale regime.
2. For most of the stations, the simulations correctly reproduce the most frequently and infrequently observed octants. In some cases the simulated most frequent octants are shifted clockwise to the nearest one, i.e., shifted by 45°.
3. All simulated winds are below 7 m/s but higher wind speeds are observed in some of the stations, in particular for the high elevation stations on the slope and in the inland.
4. At most of the stations the model reproduces fairly well the width of the wind direction distribution.
5. The model predicts quite well the observed differences in the wind direction distribution among the three groups of stations (the mountain stations, the coastal plain stations and the inland stations), i.e., the maximum and width of the distribution. These differences arise from the different mechanisms dominating the flow: mostly land-sea breeze in the coastal plain and inland stations, and additional mountain induced winds for the stations on and near the mountain.

5.3. Monthly averaged daily cycles of wind speeds.

Fig. 6 shows the monthly averaged wind speeds as a function of the day hour (local standard time) for observations and model results at each station.

The results may be summarized as follows.

1. At the low elevation stations 2, 4, 6 and 8, there is good agreement between the observations and the model results for the timing and the amplitude of the diurnal cycle.
2. At the high elevations stations 1 and 3, the model reproduces quite well the timing of the diurnal cycle but fails to reproduce the enhanced observed speeds as was pointed out in Sect. 5.2.
3. At station 7 the model predicts the maximum speed about two hours later than observed. We recall the failure of the model to reproduce the correct diurnal cycle of the temperature at this station as well.
4. In most stations the model predicts a local maximum between 5-6 am. This coincides with the minimum temperatures seen both in observations and model results at all stations at 5 am (Fig. 4). This probably indicates the arrival of the land breeze to the inland and coastal flat terrain stations, or the well developed katabatic flow along

the slope. In the next section, wind vector hodographs will indeed show easterly wind direction during these hours at the low elevation stations. However, apart from station 2, no such speed maximum is evident in the observations. This discrepancy may be due to incorrect model dynamics, or to the calm winds that are inaccurately measured.

5.4. Monthly averaged hourly wind vectors

The direction of rotation of the wind vector constitutes a tool for understanding the boundary layer dynamics and has application to dispersion and diffusion of pollutants and their possible recirculation (see for example Anthes 1978, Wever 1978).

Fig. 7 presents observed and simulated monthly averaged wind hodographs for 4 of the stations, 1, 2, 4 and 8. Each point on the segmented line (elliptic like) denotes the head of the monthly averaged wind vector at the given hour of the day (starting from the origin). Positive u and v depict westerly and southerly wind vector components respectively. The straight line starting at the origin represents the 24 hours monthly averaged wind vector. We limit the discussion to a qualitative comparison between the different stations and between observed and simulated hodographs. Moreover, we will not discuss the sense of diurnal rotation of the hodographs as the origin is not inside them and a coordinate transformation is needed (see e.g. Kusuda and Alpert, 1983). This may be a subject for future work. We summarize the comparison, which complements the discussion in previous sections, as follows.

1. Both observations and simulations show clearly different hodographs patterns for the high elevation station 1 as compared to the flat terrain stations 2, 4 and 8. Flat terrain stations show larger eccentricity of the ellipses, which indicates the difference in the dynamics: while the flat terrain dynamics are mostly determined by the sea-land breeze mechanism, the stations on the ridge are also influenced by the slope induced flow.
2. In all cases simulated ellipses are rotated clockwise (by about 30°) relative to the observed ellipses. This discrepancy seems to be a systematic error.
3. Observed and simulated ellipses at station 2 show clearly the veering of the wind by 180° late at night or very early morning hours as the land-breeze arrives. This coincides with the maximum speed at night displayed in Fig. 5 and minimum temperatures in Fig. 4.
4. The effect described in the previous paragraph is shown by model results for stations 4 and 8 as well. However, observations do not show it. As stated above, we should keep in mind the fact that calm winds are involved in these phenomena implying inaccurate measurements.

6. SUMMARY AND FUTURE WORK

We presented an evaluation of MM5 model performance at high horizontal resolution in an area of complex terrain. We emphasize the

importance of these kind of evaluations when modeled meteorological variables are to be used as input for air quality models. The evaluation is done for a specific set of model parameters and for runs with minimal input requirements, i.e., based on reanalysis data only, without performing objective analysis previous to or data assimilation during the runs. The evaluation shows that the model reproduces most of the major features that characterize the atmospheric dynamics in the area: 1. The model is able to reproduce rather well the wind direction distribution: the most frequent octants and the most infrequent octants are mostly the same in the simulations and in the observations, in some cases the most frequent octants are shifted by 45° clockwise; 2. Average simulated wind speeds show the observed diurnal cycle for most of the stations, but the model fails to reproduce the enhanced speeds observed especially at high terrain elevation stations; 3. Average simulated temperatures are in agreement with the diurnal observed cycle at most of the stations, thereby showing the effect of topography and distance from the coast; 4. Simulated wind hodographs show a similar pattern to the observed ones, showing differences between high and low topography stations, but are rotated clockwise by about 30° for most stations (root mean square errors of 45°-50° have been reported in various works dealing with MM5 simulations at high horizontal resolutions, see e.g. Hanna and Yang, 2001).

The evaluation shows that in some cases correct prediction of temperatures does not guaranty correct wind prediction: for example at some stations the model succeeds to predict the temperature correctly but fails to predict the correct wind speeds (e.g. stations 1 and 3).

The study shows that the accuracy of the model varies according to the characteristics of the terrain. Therefore, it stresses the need for detailed evaluations and verification in areas of complex terrain (in contrast to an evaluation averaged over the whole set of observation stations in the studied domain) as the discrepancies between the model results and the observations in some parts of the domain may be of critical importance. The evaluation shows the difference in timing encountered in some cases between model results and observations, which may be a crucial point when dealing with air quality. We suggest the following approaches in order to optimize model results. 1. Increase horizontal resolution in order to model correctly the complex topography and coastline. 2. Increase vertical resolution to be consistent with the high horizontal resolution (see e.g. Lindzen and Fox-Rabinovitz, 1989). In addition, some authors have argued that the planetary boundary layer parameterizations available in MM5 model tend to produce too much vertical mixing (see e.g. Mass et al., 2002) therefore giving rise to excessive geostrophic near surface winds. This could be the case when a systematic error in wind direction seems to appear. Increasing the vertical resolution will diminish the over-mixing effect. 3. Improve initial guess and lateral boundary conditions by objective analysis and perform assimilation of data from stations at locations with different terrain characteristics. 4. Adapt land use parameters to the specific area. Moreover, we are aware of the fact that including an urban surface layer parameterization and/or urban boundary layer

parameterization should improve the model performance. Some authors have implemented such schemes in MM5 (e.g. Otte and Lacser, 2001) and found basic improvements in the simulated results. 5. Some authors have pointed out the importance of using a true horizontal diffusion scheme in areas of valley-mountain topography in contrast to diffusion on the model sigma levels and implemented it in MM5 (e.g. Zangl, 2002). They found improvements in the temperature and wind prediction. 6. Check sensitivity to SST values, especially the effect on the strength of the sea-land breeze.

7. REFERENCES

Alpert, P., A. Cohen, E. Doron, and J. Neumann, 1982: A model simulation of the summer circulation from the eastern Mediterranean past Lake Kineret in the Jordan Valley, *Mon. Wea. Rev*., **110**, 994-1006.

Alpert, P., R. Abramski, and B.U. Neemman, 1992: The prevailing summer synoptic system in Israel – Subtropical high, not Persian trough, *Isr. J. Earth Sci.* **39**, 93-102.

Anthes, R.A., 1978: The height of the planetary boundary layer and the production of circulation in a sea breeze model, *J. Atmos. Sci.*, **35**, 1231-1239.

Arrit, R.W., 1989: Numerical modeling of the offshore extent of sea breeze, *Quart. J. Roy. Meteor. Soc*., **115**, 547-570.

Da-Silva, A., and P. Alpert, 1996: Documentation of the multi-year GEOS-1 assimilation data subset for the Northern Africa, the Mediterranean and the Middle East, *NASA/Goddard Space Flight Center, Data Assimilation Office Note 96-05*, 24 pp.

Doron, E., and J. Neumann, 1977: Land and mountain breezes with special attention to Israel's Mediterranean coastal plain, *Israel Meteor. Res. Papers*, **1**, 109-122.

Hanna, R.S., and R. Yang, 2001: Evaluations of mesoscale models' simulations of near surface winds, temperature gradients, and mixing depths, *J. Appl. Meteor.*, **40**, 1095-1104.

Khain, A.P., D. Rosenfeld, and I. Sednev, 1993: Coastal effects in the Eastern Mediterranean as seen from experiments using a cloud ensemble model with detailed description of warm and ice microphysical processes, *Atmos. Research*, **30**, 295-319.

Kusuda, M., and P. Alpert, 1983: Anti-clokwise rotation of the wind hodograph. Part I: Theoretical Study, *J. Atmos. Sci.*, 40, 487-499.

Lieman, R., and P. Alpert, 1993: Investigation of the planetary boundary layer height variations over complex terrain, *Bound.-Layer Meteor.*, **62**, 129-142.

Lindzen, R.S., and M. Fox-Rabinovitz, 1989: Consistent Vertical and Horizontal Resolution, *Mon. Wea. Rev*., **117**, 2575-2583.

Mass, C.F., D. Ovens, K. Westrick, and B. Colle, 2002: Does increasing horizontal resolution produce more skillful forecasts?, Bull. Amer. Meteor. Soc., **83**, 407-430.

Otte, T.L., and A. Lacser, 2001: Implementation of an Urban Canopy Parameterization in MM5 for Meso-Gama-Scale Air Quality Modeling Applications, Preprints, *9th Conference on Meso-Scale Processes, August 2001, Ft. Lauderdale, FL.,* 78-81.

Wever, M.R., 1978: Average diurnal wind variation in southwest lower Michigan, J. Appl. Meteor., 17, 1182-1189.

Zangl, G., 2002: An improved method for computing horizontal diffusion in a sigma – coordinate model and its applications to simulations over mountainous topography, *Mon. Wea. Rev.*, **130**, 1423-1432.

AKNOWLEDGEMENTS

We are grateful for helpful private communications from Dr. Ytzhak Feliks regarding the observations and their interpretation.

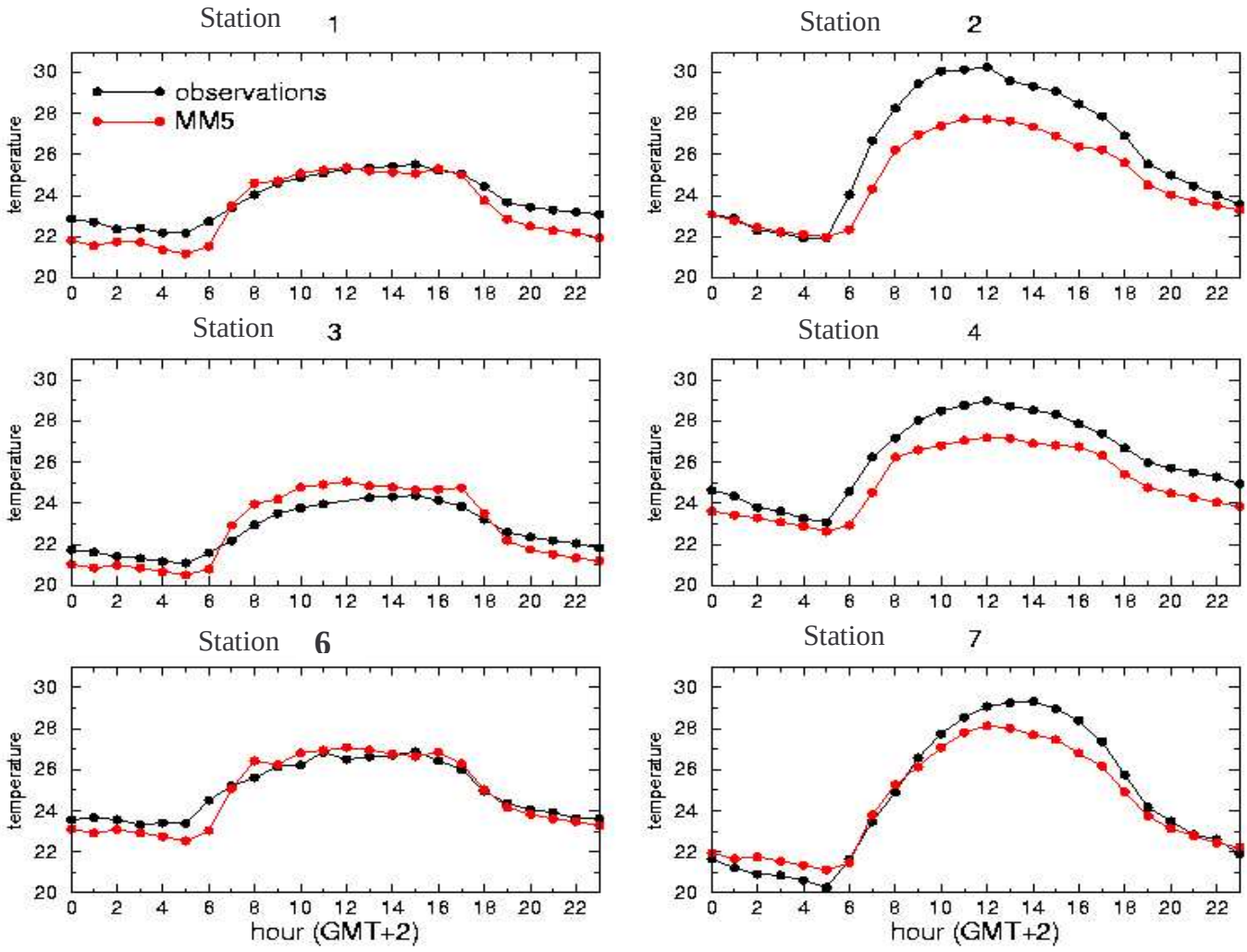

Fig. 4: Monthly averaged observed and model temperatures as a function of the local standard time for 6 of the stations (no temperature measurements were available for stations 5 and 8). Black lines: observations. Red lines: model results.

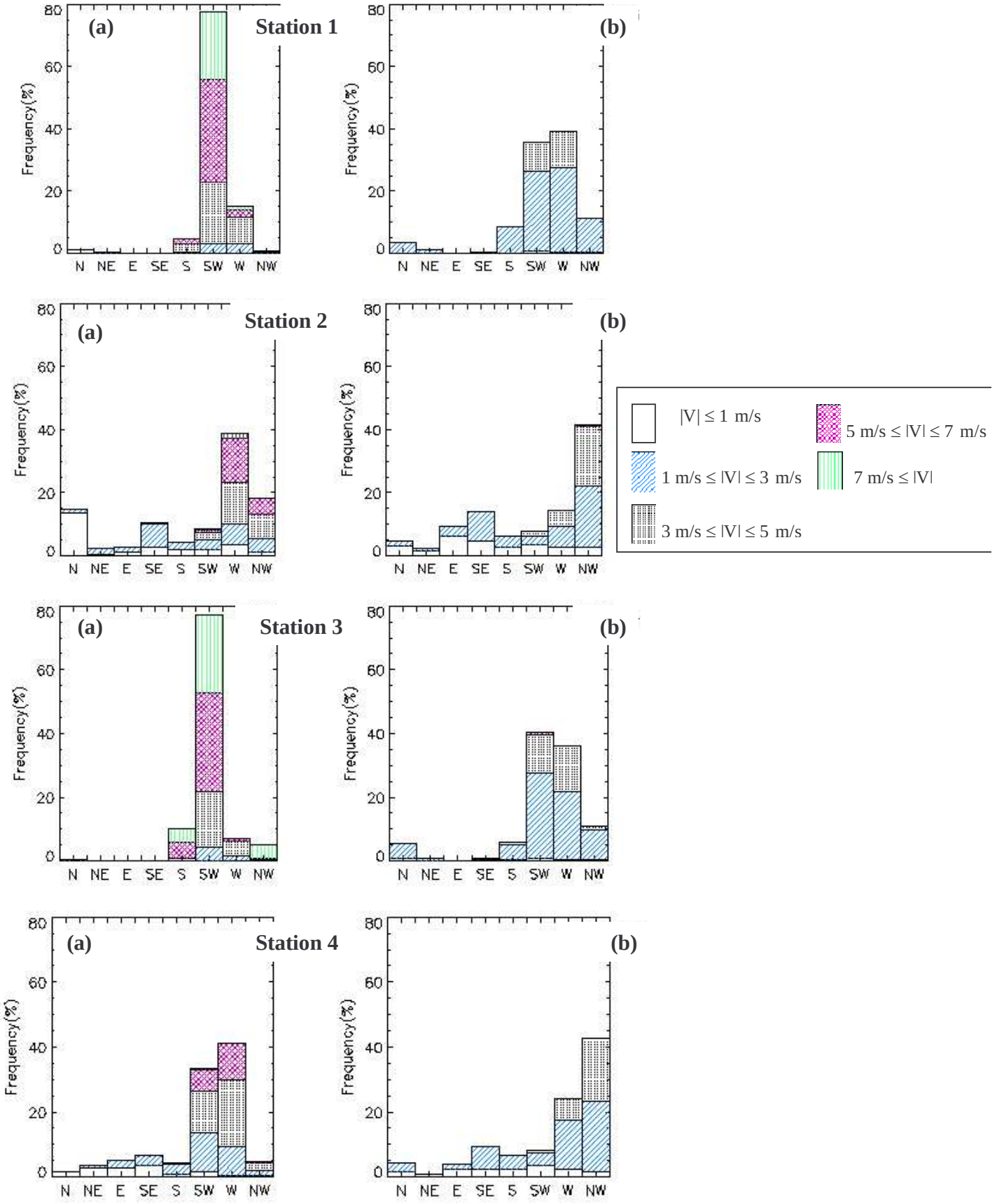

Fig. 5a: Distributions of wind direction into octants and wind speeds into 5 categories for stations 1, 2, 3, 4. (a) Observations. (b) MM5 results.

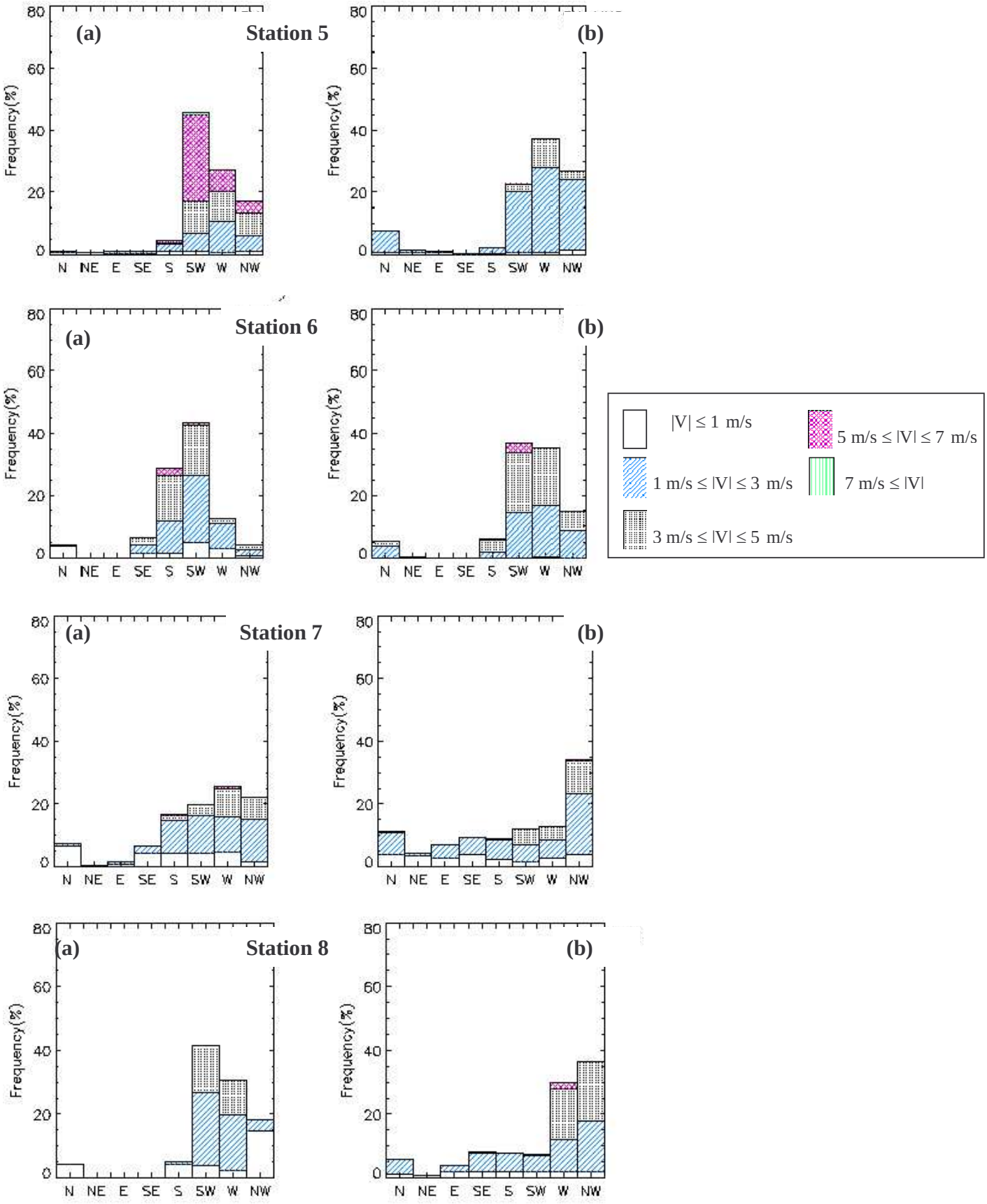

Fig. 5b: Distributions of wind direction into octants and wind speeds into 5 categories for stations 5, 6, 7, 8. (a) Observations. (b) MM5 results.

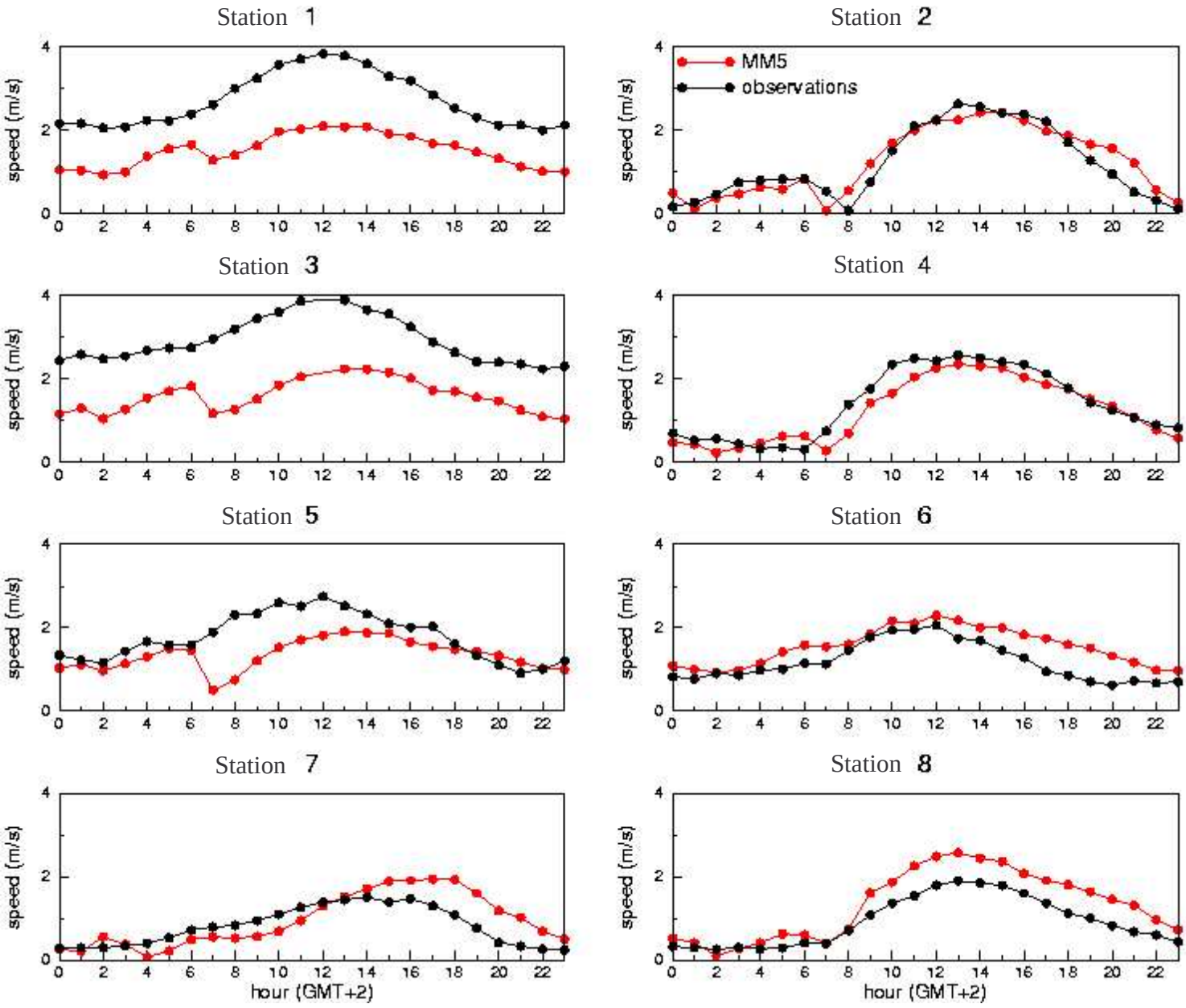

Fig. 6: Monthly averaged observed and model speeds as a function of the local standard time for the eight stations. Black lines: observations. Red lines: model results.

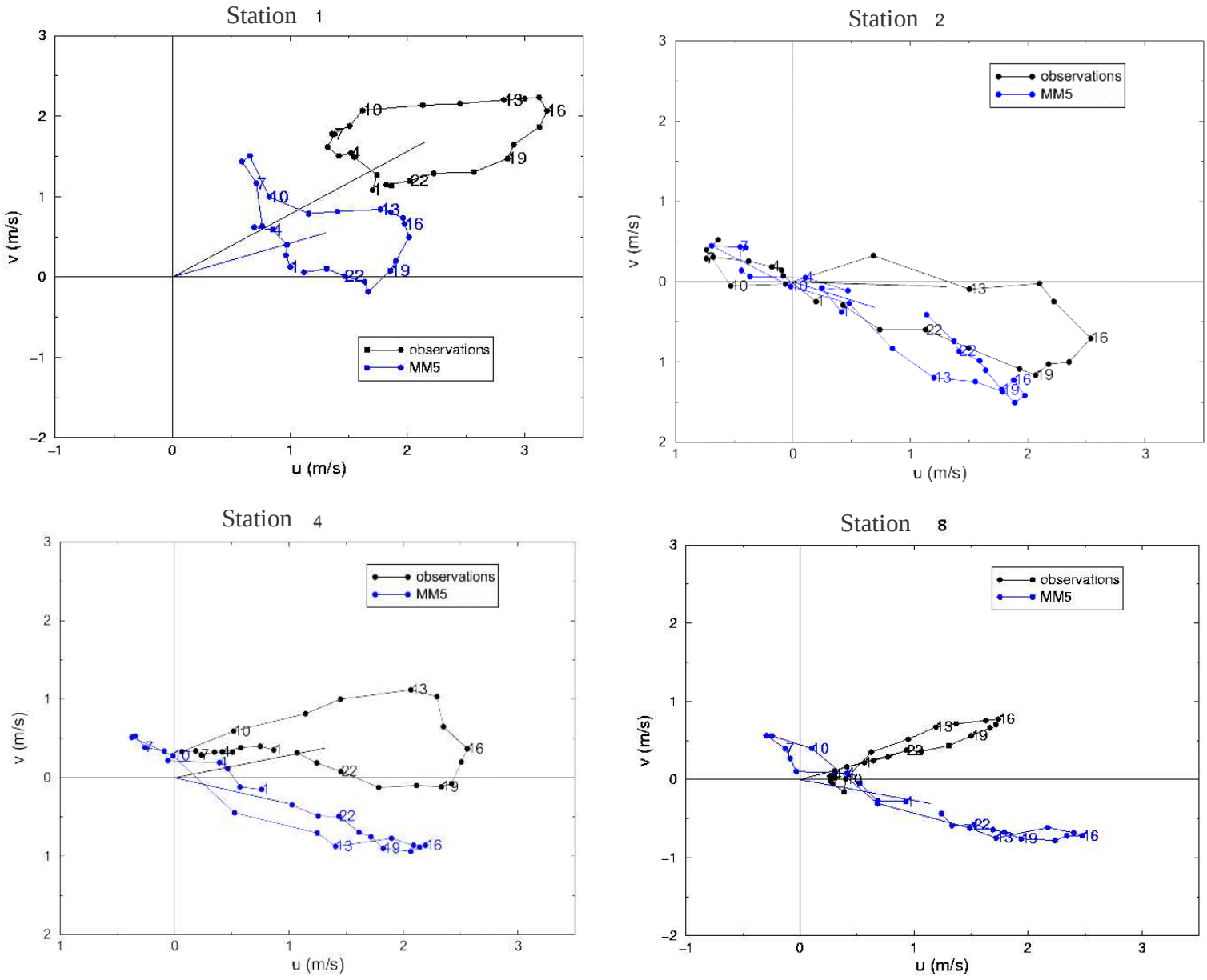

Fig. 7: Monthly averaged hodographs: Each point represents the head of the averaged wind vector at the specific hour of the day (local standard time). Straight lines starting at the origin represent the 24 hours monthly averaged wind vectors, positive u for westerly winds, positive v for southerly winds. Black lines and points: observations. Blue lines and points: MM5 model results.